

Chapter 3

Additional Sensors for Combustion Analysis



Abbreviations and Symbols

| | |
|------------|-------------------------------------|
| BMEP | Brake mean effective pressure |
| CFD | Computational fluid dynamics |
| CRDI | Common rail direct injection |
| ECU | Electronic control unit |
| EGPS | Exhaust gas pressure sensor |
| EGR | Exhaust gas recirculation |
| FM | Frequency modulation |
| LDV | Laser Doppler vibrometer |
| MR | Magneto-resistive |
| NTC | Negative temperature coefficient |
| PM | Particulate matter |
| SOI | Start of injection |
| TDC | Top dead center |
| UEGO | Universal exhaust gas oxygen sensor |
| A | Orifice area |
| d | Orifice plate diameter |
| I | Current flowing through hot wire |
| R | Electrical resistance of the wire |
| V | Airflow velocity past the wire |
| \dot{m} | Mass flow rate |
| C_d | Orifice discharge coefficient |
| n_c | Number of cylinders |
| N_m | Minimum engine speed |
| V_s | Swept volume |
| ρ | Density of air |
| ΔP | Pressure drop across the orifice |

3.1 Exhaust and Intake Pressure Sensors

Gas exchange process (gas flow into and out of the engine) affects the global engine operation, not only in the field of acoustic emissions but also in the domain of its performance and pollutant emissions. Increasingly stringent emission legislation also demands low-pressure measurement for analyzing and optimizing the gas exchange process [1]. The engine combustion process is directly affected by the gas flow dynamics in the engine combustion chamber, which is governed by the gas exchange process. Improved cylinder charging and charge motion can be achieved by optimizing the dynamic behavior of the gas flow, which is performed by low-pressure measurement and analysis [2]. A more detailed combustion analysis can be performed by understanding the charging and charge flow characteristics. The low-pressure measurement along with high-pressure measurement (in-cylinder) and valve lift can be used to determine accurate heat release during combustion. Additionally, measured exhaust and intake pressure data are typically used in the experimental analysis (e.g., calculation of residual gas fraction and trapping efficiency) and to experimentally validate the simulation data and results (1D or CFD models).

The inflow and exhaust of the engine combustion chamber (gas filling and residual gas fraction) are affected by the minor differences of pressures in the exhaust and intake manifold. Gas exchange analysis requires precise information of the manifold pressure (phase and absolute pressure value). Several factors govern the absolute pressure value and the dynamics of pressure signal in the exhaust and intake manifold, which include mounting of the sensor (flush mounting, fitting, directly or in adapter), type and performance of sensor, the radial position of the sensor and distance to cylinder head, setting of zero point (typically in warm conditions), measuring devices, and data acquisition [1]. Typically measuring inaccuracy less than 10 mbar is required for every engine test conditions. Inaccuracy of greater than 10 mbar leads to a significant error in estimation of the gas exchange phase because there exists a relationship between the gas mass flows and the absolute pressure values. Thus, the pressure must be measured by using high-precision sensors with highly sensitive measuring elements. To ensure the best possible accuracy of the measured data, any electrical (ignition, grounding, etc.) and physical (tension, temperature, gas dynamics, etc.) effects on the output signal need to be avoided.

The piezoresistive sensors are typically used for low-pressure measurement (or gas exchange). The absolute and dynamic pressure in the engine manifold is measured by piezoresistive pressure transducers. The piezoresistive pressure sensor is based on the measurement of variation in the electrical resistance of a semiconductor under mechanical load. This effect is about 70- to 150-fold greater than the strain-resistance effect exploited by metal strain gauges, which makes it possible to manufacture smaller sensors with high sensitivity and natural frequency [3]. The measuring element of a piezoresistive pressure sensor consists of a silicon load cell with a thin diaphragm, in which four resistors are implanted and connected to form a Wheatstone bridge. The registers are arranged in such a way that part of the resistors

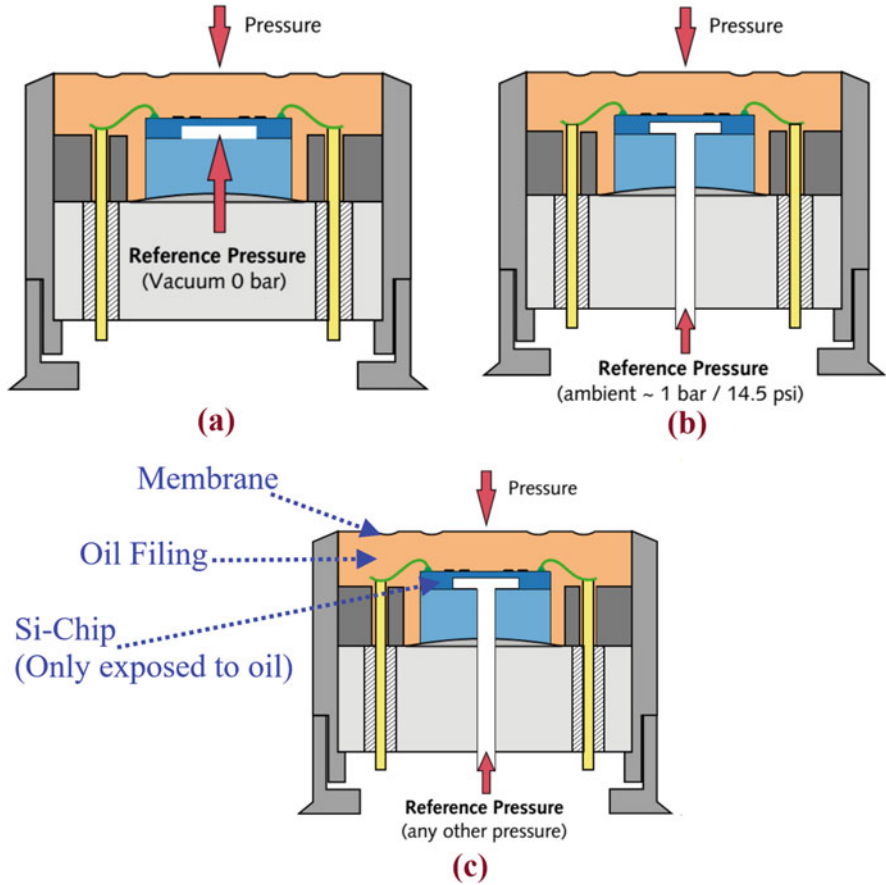
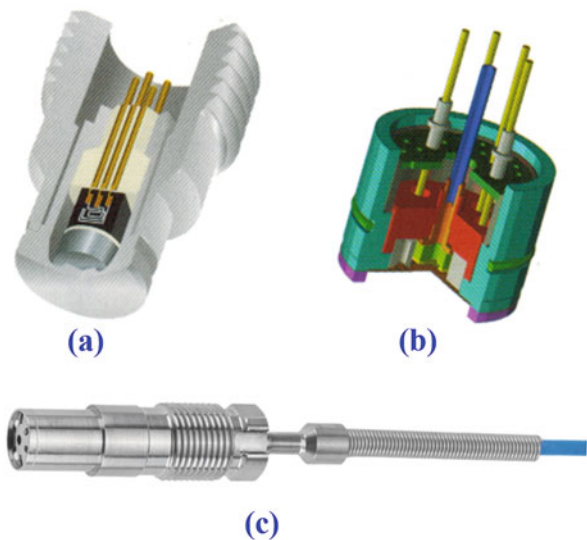


Fig. 3.1 Functional principle of the piezoresistive sensor (Courtesy of KISTLER). (a) Absolute pressure sensor, (b) gauge pressure sensor, (c) differential pressure sensor

is under tension and the rest are under pressure. The resistors are placed in the sensor chip that is integrated into the measuring cell as shown in Fig. 3.1. The pressure-dependent changes in the resistance are transformed into analog voltages by a separate electronic circuit. In recent versions, the pressure cell is integrated into the chip with “volume micromechanics” [4].

The piezoresistive pressure sensors measure the actual pressure relative to a reference pressure. The piezoresistive pressure sensors can be categorized as absolute, relative (gauge), and differential pressure sensors (Fig. 3.1). Absolute pressure sensors measure the pressure compared to a vacuum enclosed in the sensor element. Relative (gauge) pressure sensors measure the pressure in relation to the ambient air pressure. Differential pressure sensors measure the pressure difference between any two pressures. Thus, differential pressure sensors have two separate pressure connections. Depending on the application, absolute, relative (gauge), or differential pressure sensors can be suitably used.

Fig. 3.2 Piezoresistive sensors: (a) high-pressure sensor with the block-type measuring element, (b) oil-filled sensor with steel diaphragm and a measuring element with the diaphragm, and (c) actual sensor image (Courtesy of KISTLER)



An involved packaging process is used to assemble the load cells into a pressure sensor. This involves attaching the load cell to a glass plate forming a base, placing it in a case, and sealing it with a thin steel diaphragm. The pressure is transmitted between the steel diaphragm and load cell via an oil cushion [3]. Figure 3.2 shows the actual piezoresistive sensors along with the cut sections with internal details. Piezoresistive sensors are suitable for measuring static pressures.

Instrumentation of the inlet and exhaust manifold has the specific challenges for achieving accuracy and durability. An appropriate sensor can be selected based on a number of application factors including thermal load, available space, soot content in gas, vibration, required accuracy, etc. Small pressure transducers are mostly appropriate for intake manifold pressure measurement, and it can be directly installed in the intake manifold. Exhaust gas pressure sensor (EGPS) essentially required to be actively cooled because exhaust gas temperatures can be as high as 1000 °C and even above depending on engine operating conditions. These sensors typically consist of steel diaphragm and filled with oil for transferring force to the measuring cell (media separation) because of harsh media (soot, combustion gases) exposure [1].

Exhaust gas pressure sensor also plays a key role in detecting the clogging degree of the particulate matter (PM) removal filter using a pressure signal and in sending feedback to the engine control system. The exhaust gas environment is extremely humid, and, thus, the condensed water of exhaust gas is supposed to be extremely acidic in nature. Additionally, soot can be easily accumulated under such a condition. Therefore, exhaust gas pressure sensors must possess three important factors: resistance to corrosion, resistance to icing, and resistance to clogging. A highly reliable (resistive to acid, icing, and clogging) against the exhaust gas environment and compact size sensor is developed by novel soft gel with high resistance to acid and applying the gel for the original back-surface sensing structure [5].

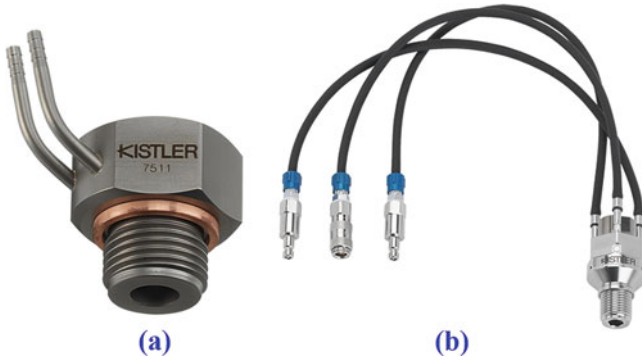


Fig. 3.3 Typical (a) cooling adapter and (b) cooled switching adapter for pressure measurement for gas exchange analysis (Courtesy of KISTLER)

The pressure sensor for gas exchange analysis has the following requirements: (1) sensor should not affect the gas exchange or combustion process; (2) sensor can be easily mounted; (3) sensor should be small size; (4) sensor should not be affected by mounting position, temperature, or vibration; and (5) sensor should have unlimited service life, and their characteristics should not change with time [3]. These factors can be considered for selection of the pressure sensor for gas exchange analysis.

Ideally during the measurement, the sensor temperature should be maintained to constant value for preventing shift in the thermal zero point. Additionally, to ensure no variation in zero-point value, the setting of zero point of the sensors can be done simultaneously. Particularly for exhaust sensors, cooling adapters are compulsory to protect the overheating of measuring element because of extremely high exhaust gas temperatures at some of the engine operating conditions. Figure 3.3a shows the typical cooling adapters for exhaust mounting of the pressure sensor. Adapters for mounting the sensor can be used with inlet and exhaust measurements, and it helps to improve the quality of measured data. A typical switching adaptor is shown in Fig. 3.3b, which fulfills some useful functions. Switching adaptor acts as a damping adaptor and effectively isolates the sensor from structure-borne vibrations, improving the quality of the output signal. Additionally, it provides cooling water channels to maintain the sensor within operational temperature limits. This feature can be useful for pressure measurement in intake as well as for exhaust manifold. Modern engines with exhaust gas recirculation (EGR) and inlet charge boosting can operate with high charge temperatures in the intake manifold also. Thus, water cooling protects the sensor and stabilizes the signal, preventing drift and significant zero offset [2]. The switching adaptor also prevents the sensor exposure to hot gas for longer than the measurement time, which extends the life of the sensor.

The sensors should be located as close as possible to the engine valves for accurate measurement. This position of the pressure sensor prevents the superimposition of gas-dynamics effects (i.e., traveling waves) on the measured pressure data. Additionally, the measuring face of the sensor should not have any dead volume in

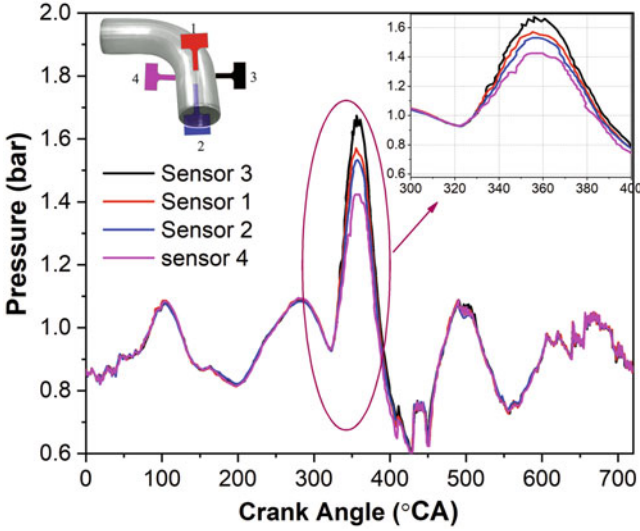


Fig. 3.4 Exhaust gas pressure signal for sensors placed on different planes at the same distance from the engine head (Adapted from [1])

front of it to avoid the pipe oscillations [2]. Flow effects in the exhaust manifold can influence the sensor signals due to the gas-dynamic oscillation in the exhaust. Hence, the installation of sensor must be selected at radial position with respect to the exhaust system geometry [1].

Figure 3.4 shows the exhaust gas pressure signal for sensors placed on different planes at the same distance from the engine head. Sensor output signals within the same measuring plane (1–2 or 3–4) show the obvious pressure differences due to the influences of the gas-dynamic effects. The differences in the pressure signals significantly occur only during the first blowoff wave [1]. The flow through the bend affected the pressure signal at position 3 (outer portion) to rise, while the pressure signal at position 4 (inner portion) is reduced considerably. The vertical position sensors 1 and 4 exhibit very small pressure differences, and, thus, no important effect is depicted due to the flow around the bend. The pressure difference between the inner and the outer walls results due to the curved flow in a bend. If required, the sensor needs to be mounted half way between the outside and inside radius for measuring the representative pressure curve [3]. The sensor should be mounted in a straight section of the manifold tube, where possible. The minimum pressure differences are obtained between the radially installed sensor and the mean pressure measured in the same plane in the case of sensors installed close to cylinder head. The sensor installed close to cylinder head has very low effect on signal differences due to the pipe geometry [1]. However, installation close to cylinder head could be critical due to availability of space. The mounting position close to the valve is no longer necessary in larger engines because of the low engine speed, no errors occur due to delays in traveling waves [3].

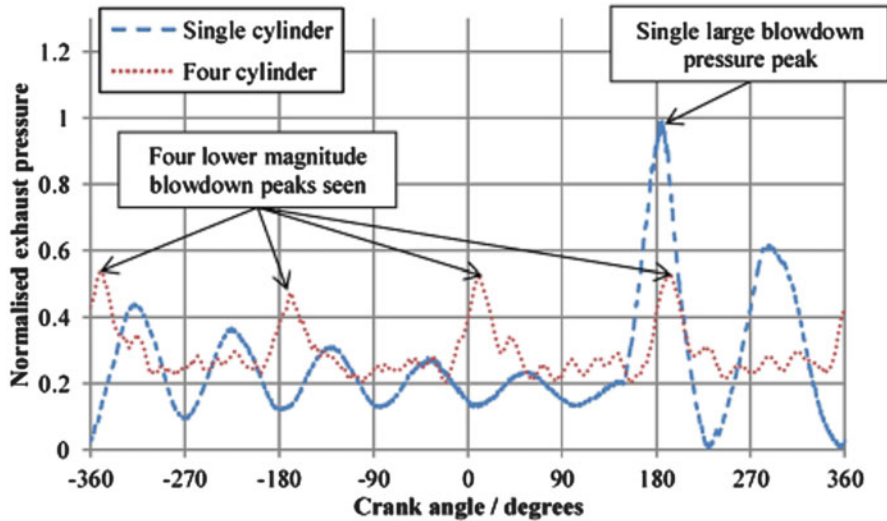
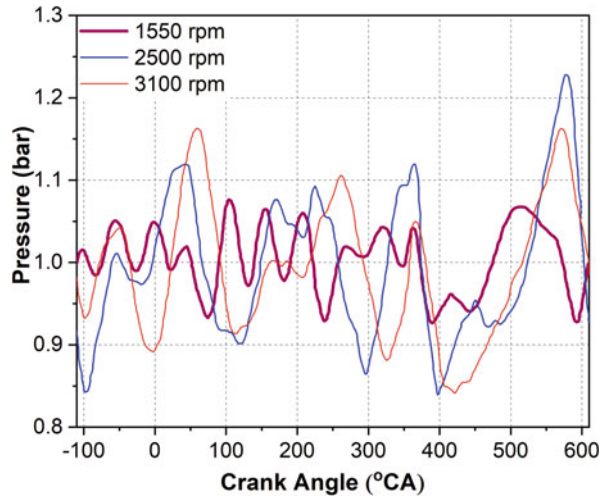


Fig. 3.5 Typical exhaust manifold pressure signal in a single- and four-cylinder engine at the same operating conditions [6]

The exhaust manifold pressure signals are significantly different for a single-cylinder engine and a typical multicylinder engine. Figure 3.5 shows the typical exhaust manifold pressure signal observed in a single-cylinder and four-cylinder engine for the same operating conditions. In the single-cylinder engine, a large single blowdown pulse is noticed at the exhaust valve opening position (Fig. 3.5). The four-cylinder engine shows four blowdown pulses which are at a much lower overall magnitude in comparison to the single-cylinder engine because of the cylinder-cylinder interactions. Optical exhaust pressure sensors are developed as an alternative to piezoresistive sensors to overcome the effect of operating temperature due to very high exhaust gas temperature [6].

Presently, tuned intake manifold is commonly used for naturally aspirated SI engines. Tuning of the manifold is performed to utilize such a manifold length which (together with intake valve opening and pressure wave exciting during the intake stroke) causes increase in the manifold pressure during intake stroke due to the interaction of pressure waves, thus improving the volumetric efficiency of the engine. In such cases, the manifold pressure signal curve will be dependent on the position of measurement and the engine operating conditions. Figure 3.6 presents the intake manifold pressure signal at different engine speeds. The lower harmonic orders have higher-pressure wave magnitude. It is also noted that not only is pressure wave amplitude magnitude important, the timing of the wave peak compared to intake valve timing is even more important, and it is better when the wave peak is located near the end of the intake stroke [7]. The impact of the distance between valves and measuring point is primarily evident in areas of rapid pressure changes. The bigger the distance, the bigger the time shift of measured signals [3].

Fig. 3.6 Comparison of measured intake pressure signal for different engine speeds at 100 mm upstream intake valve and inlet branch length 500 mm (Adapted from [7])



Accurate measurement of absolute pressure is one metrological requirement to enable correct calculation of the mass flow rates as an important part of a gas exchange analysis. The sensor must be highly sensitive to sufficiently resolve the relatively small pressure fluctuations in the inlet and exhaust manifolds. The gas fluctuations in the manifold are quite small in comparison to in-cylinder data, and, thus, high sensitivity is required to achieve a good signal-to-noise ratio.

Acceleration sensitivity is another important factor that needs to be considered for low-pressure measurement sensor. Particularly for applications in racing engines but also in production engines for vehicles, the low-pressure sensors must have the minimum possible acceleration sensitivity because the accelerations can be very substantial due to lower mass of inlet and exhaust manifolds. The accelerations of manifolds can add unwanted noise in the signal quality accordingly if it is not taken care by sensor [2, 3]. It is also advantageous to mechanically decouple the sensors from the engine with damping adapters, provided the sensors can nevertheless be mounted near the valves. Inlet pressure sensors are installed between the air cooler and cylinder in turbocharged engines. If charge temperature exceeds the sensor operating temperature or highest possible accuracy is required, sensors are installed in cooled mounting adapters (Fig. 3.3).

To lower the heating load from the sensor front, special protection screens are also used for reducing overheating. The main functions of a screen are (1) heat protection, (2) mechanical protection of steel diaphragm, (3) reduction of soot deposition in the sensor cavity, and (4) dissipation of pipe oscillation [1]. There is a distortion of the measured pressure signal depending on the design of screen and level of protection. The accuracy of low-pressure measurement also affects the cylinder pressure measurement and its further analysis, when pegging of the piezo-electric transducer is done by using a manifold pressure sensor [8].

3.2 Fuel Line Pressure Sensor

The dynamic behavior of the fuel injection system plays a key role in efficient engine operation. The fuel injection process affects the combustion process, which finally has an effect on overall fuel conversion efficiency. The time available for the fuel injection process is limited in modern high-speed diesel engines. The required fuel quantity needs to be precisely injected at the specified fuel injection timings for optimal engine performance. Thus, it is often necessary to measure the pressure in the fuel injection system of a diesel engine. Typically, fuel pressure is measured at three locations: the inlet and outlet position of the pipe conveying the fuel from the pump to injector and the fuel pressure in the injector itself [9]. The fuel injection pressure at these positions can often exceed 1000 bar in modern diesel engines. Additionally, the residual pressure between consecutive fuel injections at this position does not fall to zero (remains at a high level), due to nonreturn valve installed at the exit of the fuel pump.

Important governing factors for the selection of a fuel pressure sensor are as follows [9]. (1) Fuel pressure sensor must be small, which does not lead to significant cavities that can possibly interfere with the fuel pressure dynamics. (2) Installation of a fuel pressure sensor must not significantly alter the stiffness of the fuel line or injector. (3) Fuel pressure sensor must have sufficiently high-frequency response such that it can capture the rapid fuel pressure pulsation in the line. (4) Fuel pressure sensor must have a high natural frequency to avoid the resonant output oscillations.

Mechanical fuel injection systems (the generation before common rail fuel injection), the fuel pressure is measured between the cylinder head-mounted injector and the injector pump. Figure 3.7 presents ways for sensing the fuel line pressure by installing the sensor in the fuel line or in the injector body. A transducer boss (adapter) is welded onto the fuel pipe. A small-diameter communicating hole is then drilled through the adapter and the fuel pipe. An alternative boss (adapter)

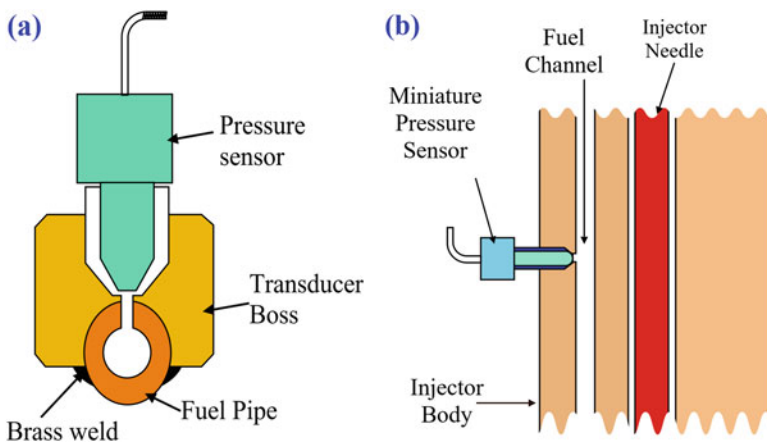


Fig. 3.7 Fuel pressure-sensing methods using sensor installation in (a) fuel line, and (b) injector body. (Adapted from [9])

Fig. 3.8 Typical adapter for fuel line pressure measurements (Courtesy of KISTLER)



design involves the clamping of the adapter onto the fuel pipe, and the fuel pressure sealing is achieved by O-rings. Typical clamping-type adapter is shown in Fig. 3.8.

The fuel pressure measurement in mechanical fuel injection system technology is straightforward. The fuel injection pressure is lower, and the line pressure is applied only during the fuel injection process. Thus, the fuel pressure in the fuel line build ups and decays in every engine cycle. Line pressure measurement can be significantly different from the combustion pressure measurement. Thermal loading is less in fuel pressure measurement, but the hydraulic pressure applied is considerable [2]. Piezoresistive sensor is typically used for measurement of fuel line pressure. Strain gauge-based pressure transducer can be also be used for measurement of fuel line pressure [9].

Figure 3.9 shows the variations of fuel line pressure at different engine load (at constant speed 1800 rpm) and engine speed (at a constant load of 6.8 bar BMEP), in an automotive engine with mechanical fuel injection system. Figure 3.9 depicts that the fuel line pressure increases with increasing engine load as well engine speed. At particular engine operating condition, the fuel line pressure builds and decays after the injection duration (Fig. 3.9). Measured fuel line pressure can be used for the evaluation of dynamic effects in the fuel injection system such as cavitation and hydraulic pressure waves.

In modern diesel engines, the common rail direct injection (CRDI) technology (latest generation) is employed, which poses new challenges for the measurement of diesel fuel line pressure [2]. The CRDI technology affects the access point available for measuring the fuel pressure. This technology is equipped with a common rail system and electronically actuated injectors. The common rail maintains continuous high-pressure fuel supply for the injectors which makes the fuel pressure independent of engine speed and load conditions. Thus, fuel quantity and fuel injection timing can be independently controlled. This technology also minimizes the

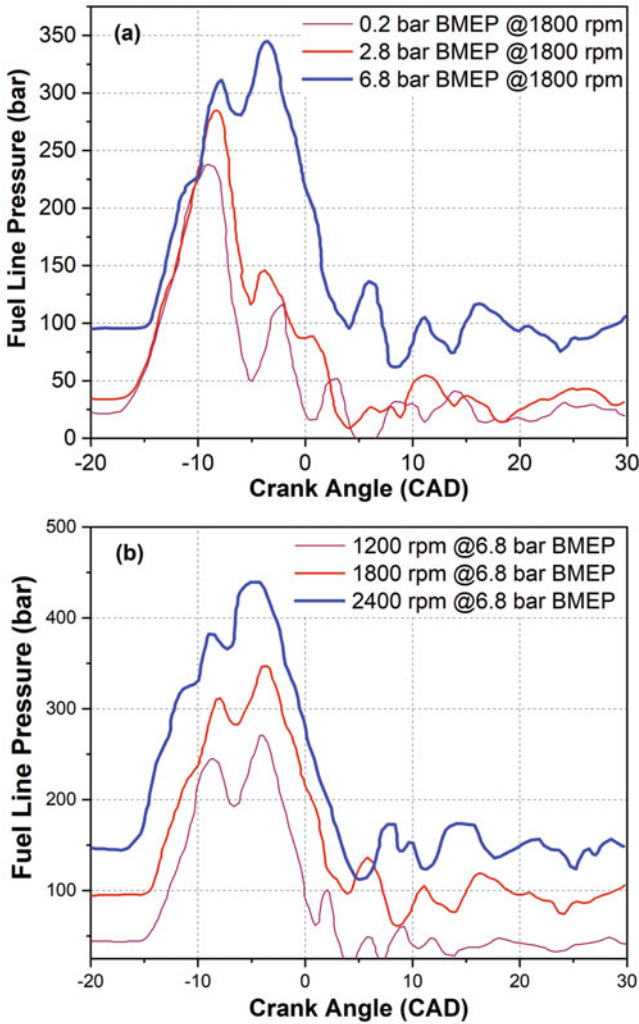
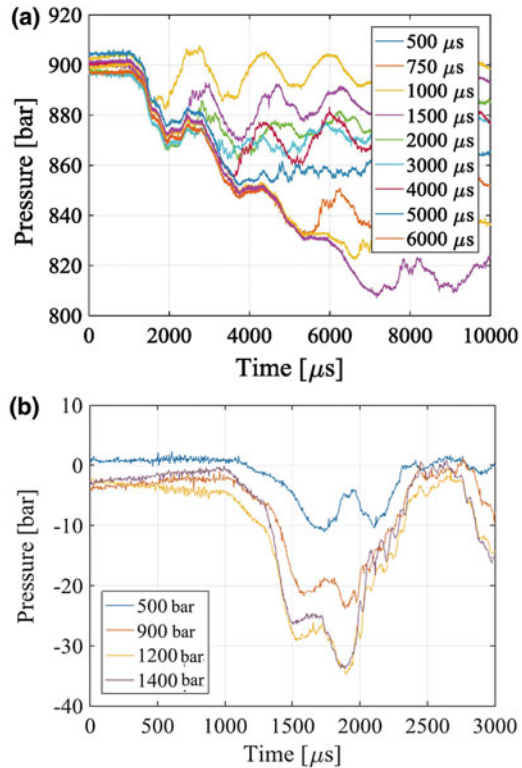


Fig. 3.9 Variations of fuel line pressure with (a) engine load and (b) engine speed, in an automotive engine with mechanical fuel injection system (Adapted from [10])

maximum pump torque requirement because high-pressure fuel delivery is achieved via common rail and peak flow rate does not require to coincide with the fuel injection event. Typically, peak pump torque is required at peak flow rate (high pressure) in a mechanical fuel injection system (Fig. 3.9). Additionally, complex injection strategy (multiple injections) can be achieved using CRDI technology to meet current and forthcoming emission legislation. The pilot fuel injection is typically used for improving the engine combustion noise. Thus, measurement of fuel pressure in CRDI is also important for understanding the pressure dynamics.

Fig. 3.10 (a) Rail pressure oscillations by needle opening and closing at different injection duration, (b) pressure drop due to fuel injection at different fuel injection pressures [11]



The quick closing and opening of the injector needle lead to high-frequency and high-amplitude fluid transients in the high-pressure common rail system [11]. While analyzing the measured fuel pressure data of CRDI system, understanding of the pressure wave propagation behavior is essential. The wave generated by one injector can affect other injectors and pipelines of the common rail system during pressure wave pressure propagation through a common rail circuit. In a high-pressure common rail system, the inertial effects of the fluid are typically more dominant than in the conventional hydraulic systems. Figure 3.10a shows the typical common rail pressure oscillations generated by fuel injections of different durations (500 μs –6 ms). The pressure oscillation either strengthens or attenuates at different fuel injection durations. Figure 3.10b shows the drop in common rail pressure by injection at different fuel injection pressures (500–1400 bar). The pressure drop is typically higher for higher fuel injection pressure (Fig. 3.10b).

The real CRDI system consists of a high-pressure pump, pressure-regulating valve, several injectors, and other components. The pressure oscillations to the fluid flow can be generated even at a distance from the original source. Thus, signal filtering is required to differentiate various sources of flow transients and to attenuate the pressure oscillation generated by injector needle closing and opening events. The detailed analysis of attenuated injection event can be used to estimate

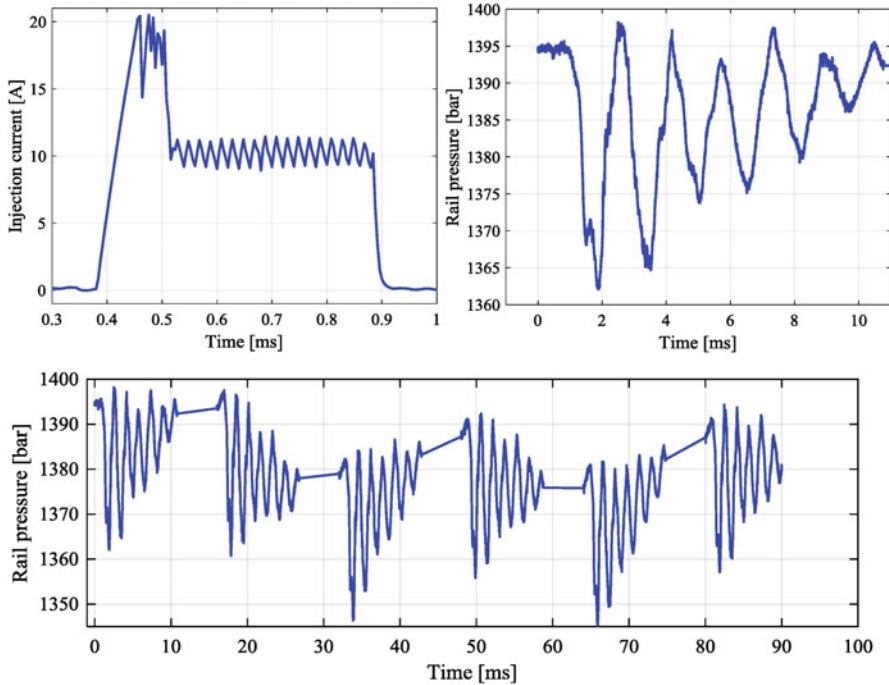


Fig. 3.11 Typical injector current, rail pressure after a single injection and six injections with 16 ms time between injections [11]

the fuel injection duration [11]. Figure 3.11 shows the typical pressure drop along with their oscillations because of the fuel injection event and corresponding control current of the injector. A six-injection event (corresponding to complete engine cycle) is also shown in lower part of Fig. 3.11. In every injection event, fuel from the common rail is injected into the combustion chamber by the injector, which suddenly drops the rail pressure (Figs. 3.10 and 3.11). This phenomenon as a feature of fuel injection and its pattern can be used to determine the duration of the injections.

3.3 Needle Lift Sensor

The movement of injector needle is frequently measured in a diesel engine to determine the start of fuel injection in the cylinder. Needle lift signal can also help in the identification of multiple injections in a particular engine cycle. The determination of the start of injection allows calculating the ignition delay, which plays an important role in diesel engine combustion. Additionally, needle lift and line pressure measurements are useful in the calculation of the fuel injection rate and identification of the dynamic behavior of fuel in the high-pressure fuel system at

different engine operating conditions. The flow in the injector nozzle is strongly influenced by the internal geometrical factors of the nozzle and the motion of the injector needle. The needle motion inside diesel injector nozzle plays a decisive role for the spray dynamics [12–16]. The turbulence level in the nozzle flow affects the spray dynamics. The turbulence kinetic energy is mainly created (independent of presence or absence of cavitation) in the first stages of injector needle opening and in the last stage of closing due to the local acceleration of the flow at the nozzle inlet generated by the restricted passage. The turbulence level significantly decreases with the increase in inlet area and stabilizes at high needle lifts (over 150 μm) and starts increasing again when the injector needle descends below 150 μm , although to a lesser extent [13]. The lift profile of injectors affects the vapor penetration length in the chamber [12]. The injector needle lift profile has a significant effect on the amount of fuel injected and the momentum of the diesel jet.

Typically, the fuel injector is instrumented for the measurement of needle lift. Several production diesel engines operating on electronically controlled diesel pumps are equipped with instrumented injectors to determine the fuel injection timings [2].

Figure 3.12 shows the typical needle lift measurement method by means of variable inductance system, which operates on a frequency modulation (FM) principle. The inductive sensor coil is part of an electronic oscillator circuit that functions at 2 MHz frequency (approximately). The frequency of oscillator is partly determined by the inductance of the sensor coil. The armature rod penetrates further into the sensor coil when the injector needle rises, which leads to the variation in inductance of coils and its oscillation frequency. The variation in oscillation frequency is captured by an electronic circuit, which converts it into the variation of output voltage [9]. The electronics of the circuit is designed in such a way that output voltage varies linearly with the injector needle lift. Figure 3.12b shows the method for incorporating the sensor coil into the fuel injector. The frequency modulation method can also be used with a sensor that relies on the variation in the capacitance (Fig. 3.12a).

For the estimation of the injector needle lift position, other types of sensor including Hall-effect semiconductors and differential transformers are also used [2, 9]. The basic requirement is to generate a signal of sufficient accuracy and repeatability, with favorable signal-to-noise ratio and acceptable durability for the application.

Figure 3.13 illustrates the typical injector needle lift profiles at several injection-pulse durations for different fuel injection pressures. The start of injection (SOI) indicates the start of sending injection-triggering signal. The needle lift profile consists of two stages, namely, the opening stage and the closing stage. The needle lift profiles of different injection-pulse durations highly overlap in the opening stage of the injector needle. The period of needle opening stage nearly equals to the duration of injection pulse. The injector needle opening speed increases at a higher injection pressure, and the needle lift is also the higher. The needle dynamics is not altered by increasing the duration of injection pulse because duration only decides the timing of opening and closing of the fuel release valve. Figure 3.13b shows the

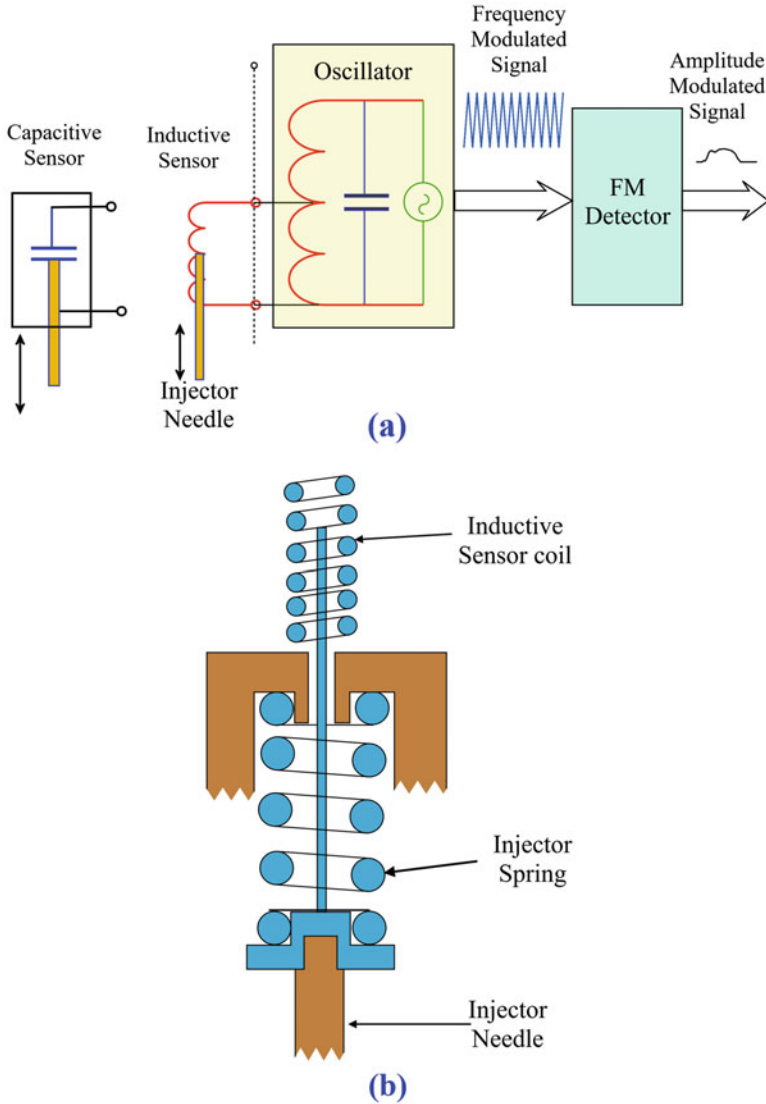


Fig. 3.12 (a) Typical needle lift-sensing methods, (b) installed sensor coil on fuel injector (Adapted from [9])

injector needle speeds for two fuel injection pressures. Abrupt velocity peaks appear at the beginning and closing of the needle movement (Fig. 3.13b). The injector needle opening speed is a function of the fuel injection pressure. The needle opening speed increases at the higher fuel injection pressure, and the needle closing speed is unaffected by fuel injection pressure (Fig. 3.13b) [15].

Figure 3.14 shows the variation of axial jet velocity (represents liquid-jet dynamics) with different needle lift profiles for two different fuel injection pressures. The

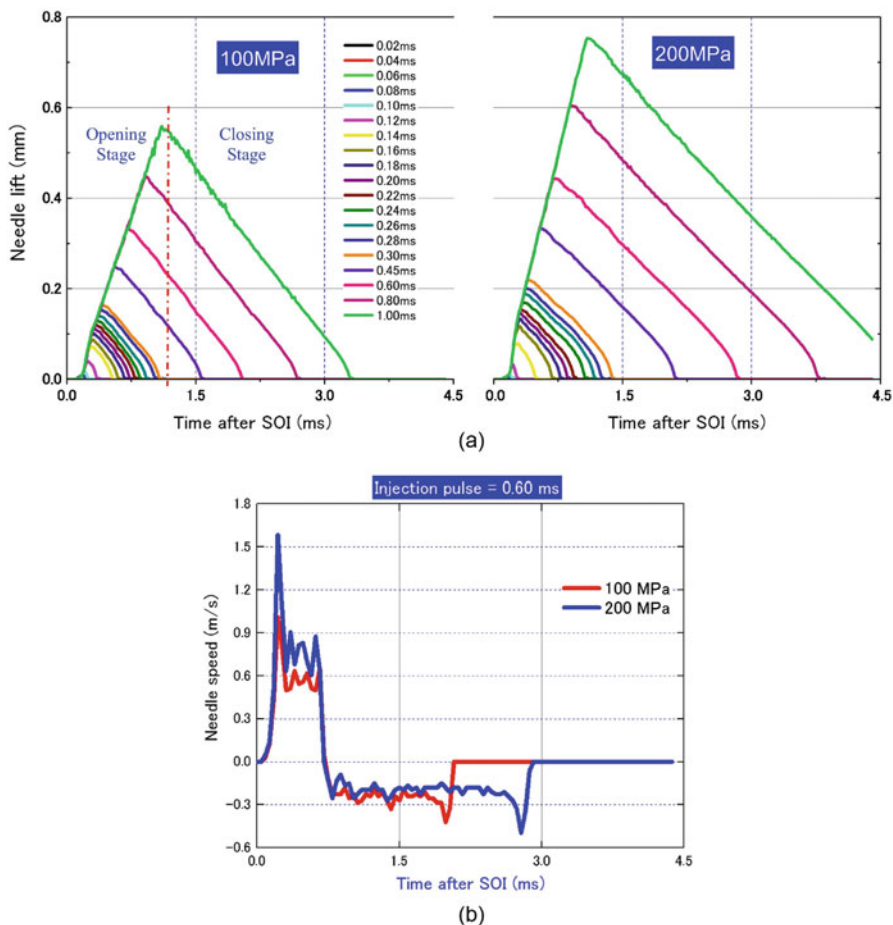


Fig. 3.13 Typical (a) injector needle lift profiles and (b) needle lift speed at different injection-pulse durations [15]

axial jet velocity profiles for different injection-pulse durations overlap with each other (Fig. 3.14). Axial jet velocity increases exponentially in the beginning at needle opening stage independent of the injection-pulse duration, and it reaches to a constant value after a particular needle lift value (Fig. 3.14b) for both the fuel injection pressures. Then after the needle reaches a certain critical height, the axial velocity becomes constant and steps into the steady state. The steady-state axial velocity increases with the increase in fuel injection pressure, but the trend of variation of axial velocity is similar (Fig. 3.14).

Typically, commercially available eddy-current sensors are used for measurement of injector needle lift position in modern electronic fuel injectors [17]. However, the repeatability and accuracy of the output signal are significantly affected by the presence of an electromagnetic disturbance. Modern electronic diesel injectors

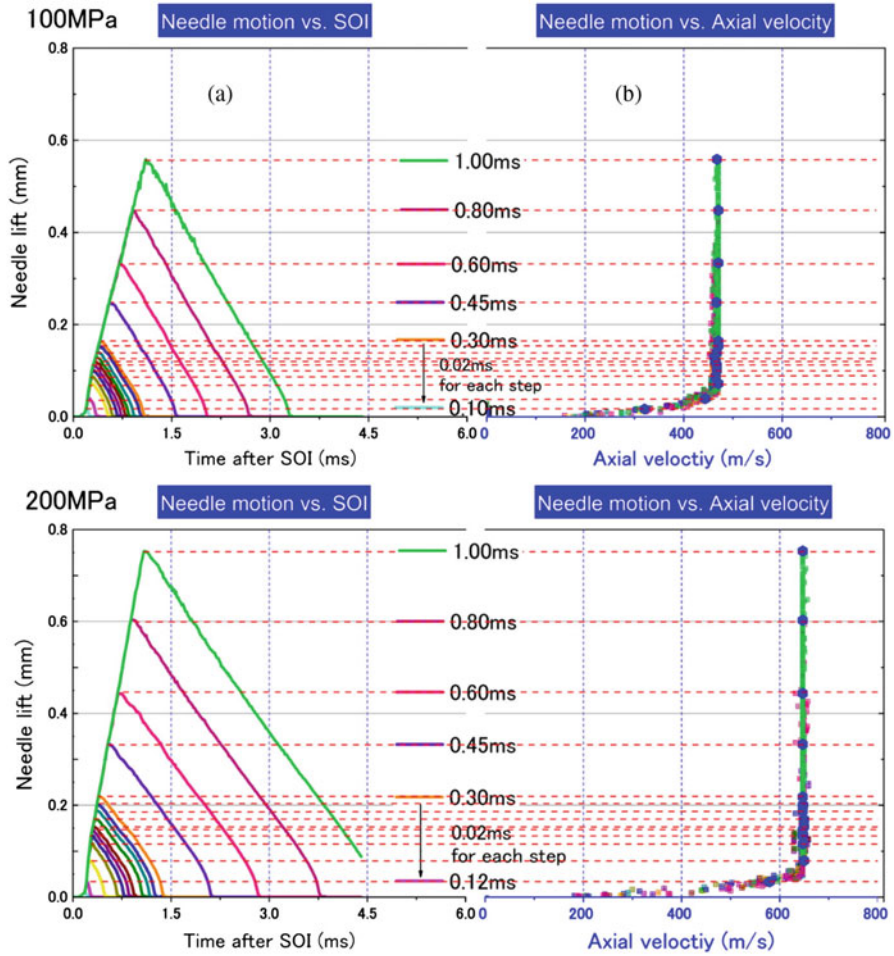
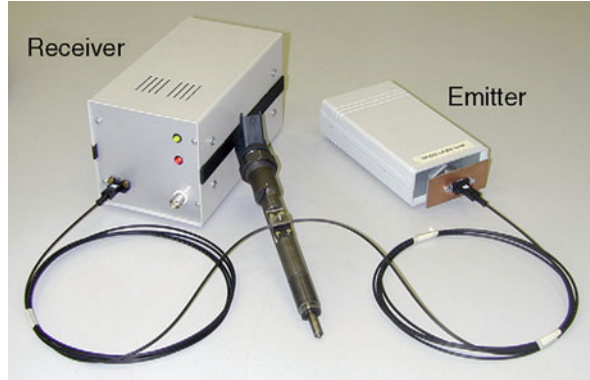


Fig. 3.14 Variations of axial jet velocity with needle lift for two different fuel injection pressure (a) needle motion with different start of injection (SOI), and (b) needle motion with axial jet velocity [15]

are typically actuated by providing high currents into a solenoid, which creates high electromagnetic fields. Additionally, the high levels of electromagnetic noise are produced by the several engine assistance devices; the measurement of injector needle lift can be very difficult with eddy-current type transducers. To overcome these issues, optical sensors are also developed for the measurement of needle lift of fuel injector [18, 19]. Figure 3.15 shows the typical optical transducer assembly on the test fuel injector. The optical sensor for needle lift measurement consists of a laser light emitter, a receiver, and a device used for modulating the intensity of the light reaching the receiver as a function of the position of moving element of the fuel injector. To get a clearance area that varied linearly with injector needle position, two rectangular windows are mounted on the injector body, while a third window is

Fig. 3.15 Typical optical transducer assembly on the test injector [18]



rigidly connected to the needle control piston and aligned with the fixed ones [18]. An optical fiber cable is used to transfer the laser lights between input and output. Light intensity is converted into an equivalent voltage signal that can be recorded and analyzed further for the determination of injector needle lift position.

3.4 Mass Flow Sensors

The mass flow measurement of air and fuel consumptions is an integral part of the combustion measurement and analysis of internal combustion engines. The measurement of air and fuel allows the calculation of various performance and combustion parameters such as air-fuel ratio, combustion efficiency, fuel conversion efficiency, volumetric efficiency, residual gas fraction, etc. These parameters are helpful in analyzing the combustion quality and determination of optimal engine operations, and, thus, air and fuel mass flow rates are often measured during engine testing.

Figure 3.16 shows the different methods for airflow measurement in reciprocating engines. Typically, one of the two airflow rate measurements, i.e., instantaneous and quasi-steady, is required for engine research. The airflow is a highly unsteady process during the intake stroke of the engine. The airflow rate varies from zero to maximum value, and again comes back to zero within a combustion cycle (few milliseconds). Measurement of instantaneous airflow rate requires specialized fast-response measuring equipment. More often average airflow rate (quasi-steady flow rate) over the entire combustion cycle is required, which can be measured in a number of ways [9]. The systems for estimating the amount of air drawn in by the engine can be divided into measuring procedures based on either volume or mass basis.

The air-box method is the simplest method that is typically used for average airflow rate measurement (Fig. 3.16a). The air consumed by the engine from the air-box is filled by atmospheric air, which enters through a calibrated orifice meter or

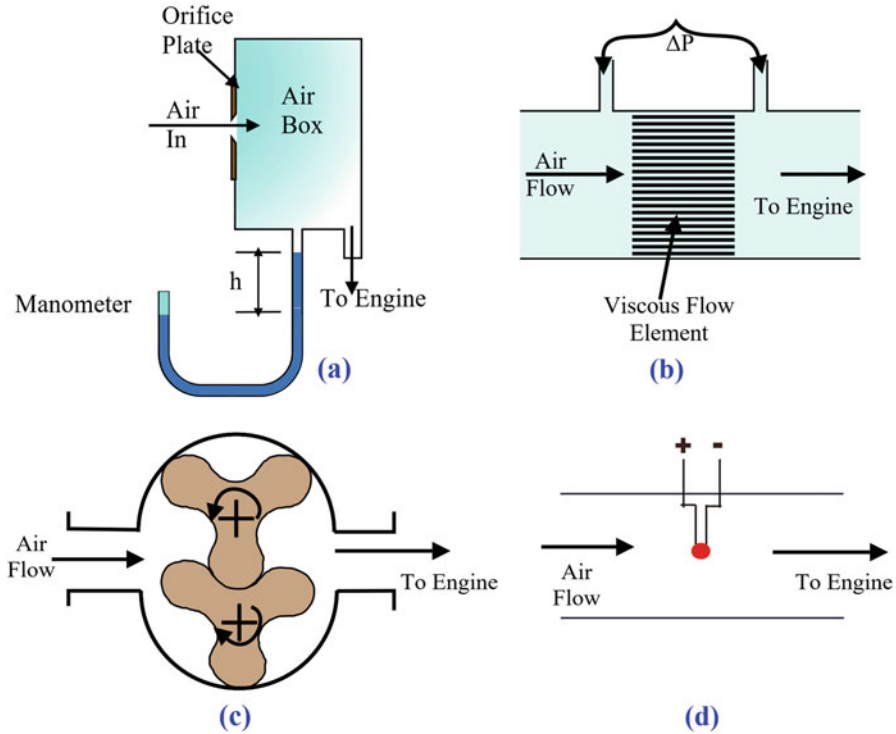


Fig. 3.16 Airflow measurement methods in reciprocating engines (a) air-box method, (b) viscous flow meter, (c) positive displacement flow meter, and (d) hot-wire flow meter (Adapted from [9])

a venturi. The volume of air-box needs to be sufficiently large to damp out the oscillating flow produced by the engine. The air mass flow rate (\dot{m}) by the orifice plate can be calculated using Eq. (3.1):

$$\dot{m} = C_d A \sqrt{2\rho\Delta P} \tag{3.1}$$

where C_d is the orifice discharge coefficient, A is the orifice area, ρ is the density of air, and ΔP is the pressure drop across the orifice. The Eq. (3.1) is applicable for incompressible flow, and it is better to limit the pressure drop (ΔP) below 1.2 kPa for good accuracy by selecting the appropriate design of orifice plate [9].

If the pressure drop across the orifice plate is oscillating, then mass flow rate will also be oscillating and not steady. In such case, the accurate mass flow determination is difficult and leads to an error in air mass calculation. Therefore, a larger box volume in conjunction with orifice plate is required to eliminate the error due to the pulsating nature of the flow in the intake manifold of the reciprocating engines. The required volume of air-box for steady flow through the orifice can be estimated using Eq. (3.2) [9, 20]:

$$V_b = \frac{417 \times 10^6 n_s^2 d^4}{n_c V_s N_m} \quad (3.2)$$

where n_s is constant (with value 1 for two-stroke and 2 for four-stroke engine), d is orifice plate diameter (m), n_c is the number of cylinders, V_s is engine total displacement volume (m^3), and N_m is the minimum engine speed of the measurement (rpm). It can be noted that the volume of air-box is dependent on the orifice diameters, so both can be selected as per requirement. A significant disadvantage of air-box is a long tube that is often required to connect with the engine, which affects the breathing characteristics and performance of the engine [9, 21].

Viscous flowmeter is another meter that is another method of quasi-steady airflow measurement as illustrated in Fig. 3.16b. In this method, the air passes through a honeycomb of narrow parallel passages so dimensioned that the flow is viscous, the resistance of the element thus being directly proportional to the velocity within the working range. The meter requires calibration against a particular standard [20]. In principle, the flow-through instrument is laminar, and pressure drop across the meter is proportional to the airflow velocity or volumetric flow rate through meter. Typically viscous flowmeter is more suitable for use in pulsating flows than an orifice plate. The demerit of this method is its sensitivity to fouling of small flow area passages, which changes the calibration [9].

Airflow measurement using a positive displacement meter is illustrated in Fig. 3.16c. This method is largely suitable only for stationary engine operation because of their distinct inertia to change in airflow [4]. The accuracy of the positive displacement meters is not susceptible to pressure oscillations in the flow.

The most significant method of the air mass flow rate measurement is the hot-film anemometer, which can measure the instantaneous air mass flow rate. The functional principle of this method is illustrated in Fig. 3.16d. The wire is maintained at higher temperature by means of electrical supply. The heat loss rate can be calculated from energy supplied to the wire, which is also related to the air mass flow rate through the flowmeter by Eq. (3.3) [9]:

$$q = I^2 R = a + b(\rho V)^n \quad (3.3)$$

where q is the heat loss rate from the hot wire, I is the current flowing through hot wire, R is the electrical resistance of the wire, ρ is the air density, V is the airflow velocity past the wire, and a , b , and n are the constants estimated by calibration of the instrument. The hot-wire flowmeters can respond almost instantaneously to the variations in the airflow rate. The hot-wire thermal inertia should be very small for fast response, and, thus, the wire diameter must be very small ($<100 \mu\text{m}$) [9].

Continuous and discontinuous volumetric as well as gravimetric measurement methods are known for measuring the fuel consumption of internal combustion engines. The volume of fuel consumed by the engine is calculated in the volumetric measurement methods. The temperature-dependent fuel density must be taken into account for the determination of the mass of fuel consumed in case of volumetric

measurement method. In contrast, the gravimetric measuring procedure directly calculates the mass of fuel consumed, and, thus, the additional uncertainty of determining the density is not required [4]. Several methods for fuel mass flow measurement are available, and the most suitable method for a particular application can be selected. The following factors can be considered for the selection of mass flowmeter: (1) volumetric or gravimetric, (2) the sensitivity to temperature and fuel viscosity, (3) absolute level of accuracy, (4) pressure difference required to operate, (5) wear resistance and tolerance of dirt and bubbles, (6) suitability for stationary/in-vehicle use, and (7) analog or impulse-counting readout [22].

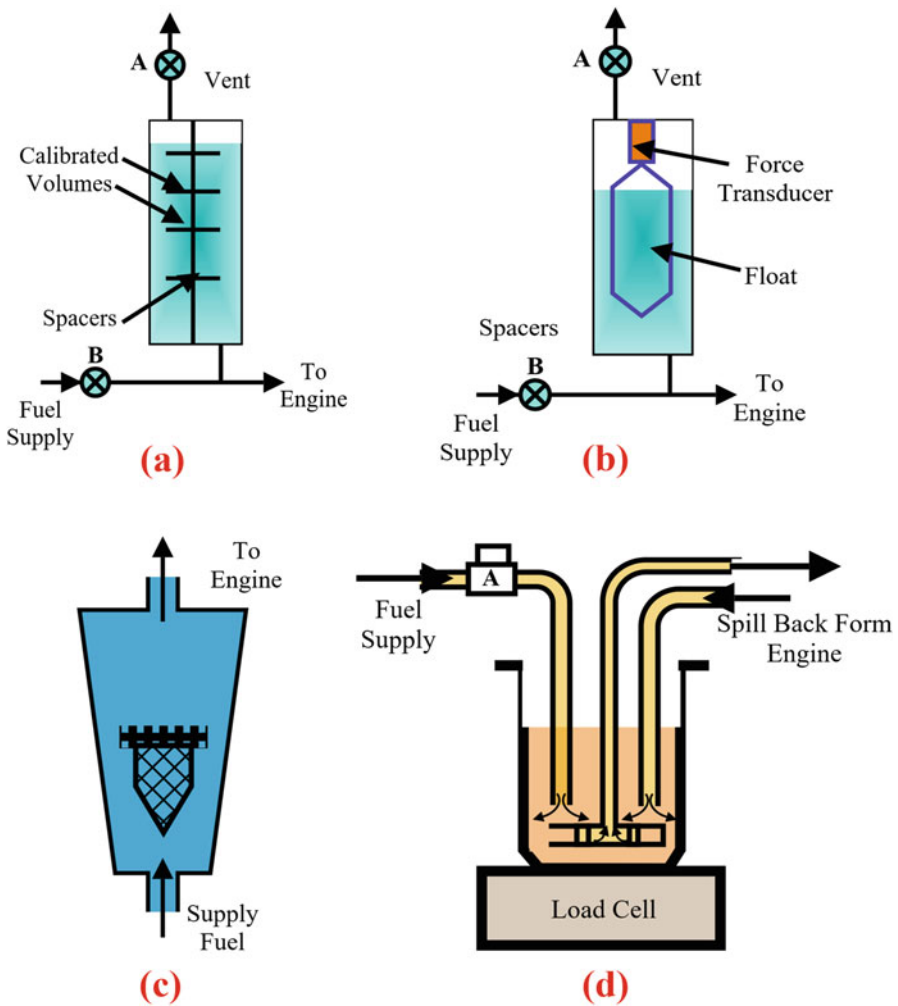


Fig. 3.17 Fuel flow measurement in reciprocating engines using (a) calibrated burette method, (b) cylindrical float based method, (c) rotameter based method, and (d) weighing (average gravimetric fuel consumption rate) method (Adapted from [9])

Figure 3.17 shows the different methods for average fuel flow rate measurement in reciprocating engines. The burette method of fuel flow rate for measuring the average fuel flow rate is illustrated in Fig. 3.17a. This method relies on the recording the time taken (by stopwatch) for consuming a particular amount of fuel by the engine. The burette is selected based on the choice of calibrated volumes in such a way that a larger calibrated volume be chosen at higher fuel consumption operating conditions. Figure 3.17b shows a method of measuring the average gravimetric fuel consumption rate. The advantage of this method is that it directly measures the mass of fuel consumption, not the volume. In this method, a cylindrical float is positioned inside a cylindrical vessel, and the buoyancy force is measured by a force transducer. The change in buoyancy force due to fuel consumption is directly proportional to the mass of consumed fuel [9]. A variable area flowmeter or “rotameter” can also be used (Fig. 3.17c), when great accuracy is not required. In this meter, a short conical float is free to move up or down a tapered transparent tube. The extent of rising of float provides an indication of the flow rate through the meter within an accuracy of a few percent. Figure 3.17d shows a weighing method for measuring the average gravimetric fuel consumption rate. The weight of fuel in the vessel at any instant can be measured using the load cell. The mass of fuel consumed by the engine over a period of time can be measured using this method.

Typical, gravimetric fuel flow measurement method includes the Coriolis and Wheatstone bridge-based devices according to the continuously measured flow principle. The method works according to the vessel principle, such as the drainage weight measurement and the weight measurement using burets and the weight principle. The continuously working mass flowmeters need the bubble separators to deaerate the approach flow and return flow. Gas bubbles in the fuel that have not been separated reduce the quality of the measuring signal and diminish the accuracy and dynamics of the system [4].

Figure 3.18 shows the schematic of the fuel mass flowmeter based on Coriolis effect. In this device, the fuel flows through the pipe sections that are electromagnetically stimulated to oscillate, with the result that the pipes are twisted because of

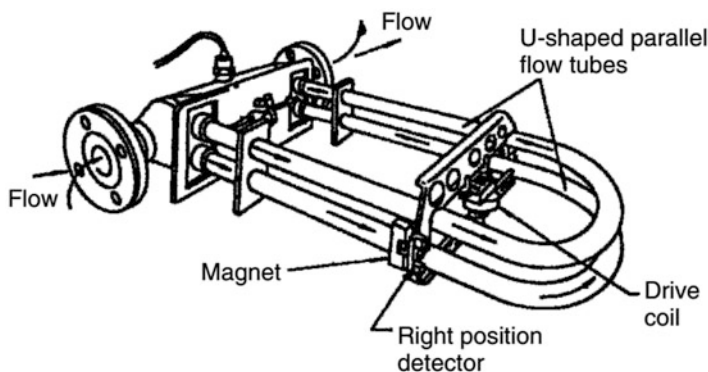


Fig. 3.18 Coriolis effect fuel flowmeter [22]

the Coriolis effect. The twist angle is calculated proportionally to the mass flow rate [4, 22]. Gravimetric methods of fuel mass determination are preferred over the volumetric methods for better accuracy of results.

3.5 Temperature Sensor

The engine management system uses several temperature inputs to improve the performance of the engine, control the emissions, and optimize the fuel conversion efficiency [23]. The most common applications for temperature sensing along with their typical measuring range are as follows: engine/coolant temperature ($-40 \dots +130$ °C), intake air temperature ($-40 \dots +120$ °C), engine oil temperature ($-40 \dots +170$ °C), fuel temperature ($-40 \dots +120$ °C), and exhaust gas temperature ($-40 \dots +1000$ °C) [23, 24].

The coolant temperature sensor measures the coolant temperature, which is used by engine management to calculate the engine temperature for achieving the optimal engine operation. The intake air temperature sensor is installed in the intake tract. This signal is used for calculation of the intake air mass together with the signal from the boost pressure sensor. The intake air temperature is often integrated with the mass flow sensor or manifold absolute pressure sensor [23]. Additionally, the desired values for the various control loops (e.g., EGR, boost pressure control) can be adapted to the air temperature. Exhaust gas temperature measurement is an emerging application of temperature sensing due to aftertreatment technologies.

A wide range of temperature-sensing technologies is available such as resistive temperature transducers, thermistors, thermocouples, PN junction sensors, liquid crystal temperature sensor, heat flux gauges, etc. [23]. A temperature-sensing technology can be selected based on the application. Typically for engine temperature measurements, a temperature-dependent semiconductor measuring resistor of the NTC (negative temperature coefficient) is installed inside a housing, a sharp drop in resistance occurs when the temperature rises in NTC-type sensors. The measuring resistor is part of a voltage divider circuit to which 5 V is applied. Thus, the measured voltage through the measuring resistor is temperature-dependent. The engine management ECU estimates the particular temperature to every resistance or output voltage based on a calibration curve stored in it [24].

3.6 Valve Lift Sensor

The continuous development of internal combustion engines increasingly demands control on the gas exchange process. The gas exchange process is mainly governed by the valve train system, which influences the combustion behavior and power output of the engine. The necessary valve lift curve must be ensured within the whole operation range of the engine along with minimum friction [25]. The measurement of valve motion during the development of engine cylinder heads and in related

component testing environments is typically required. Additionally, the fundamental research experiments may need the determination of valve motion in a running engine. The valve lift measurement is similar to the needle lift measurement, and,

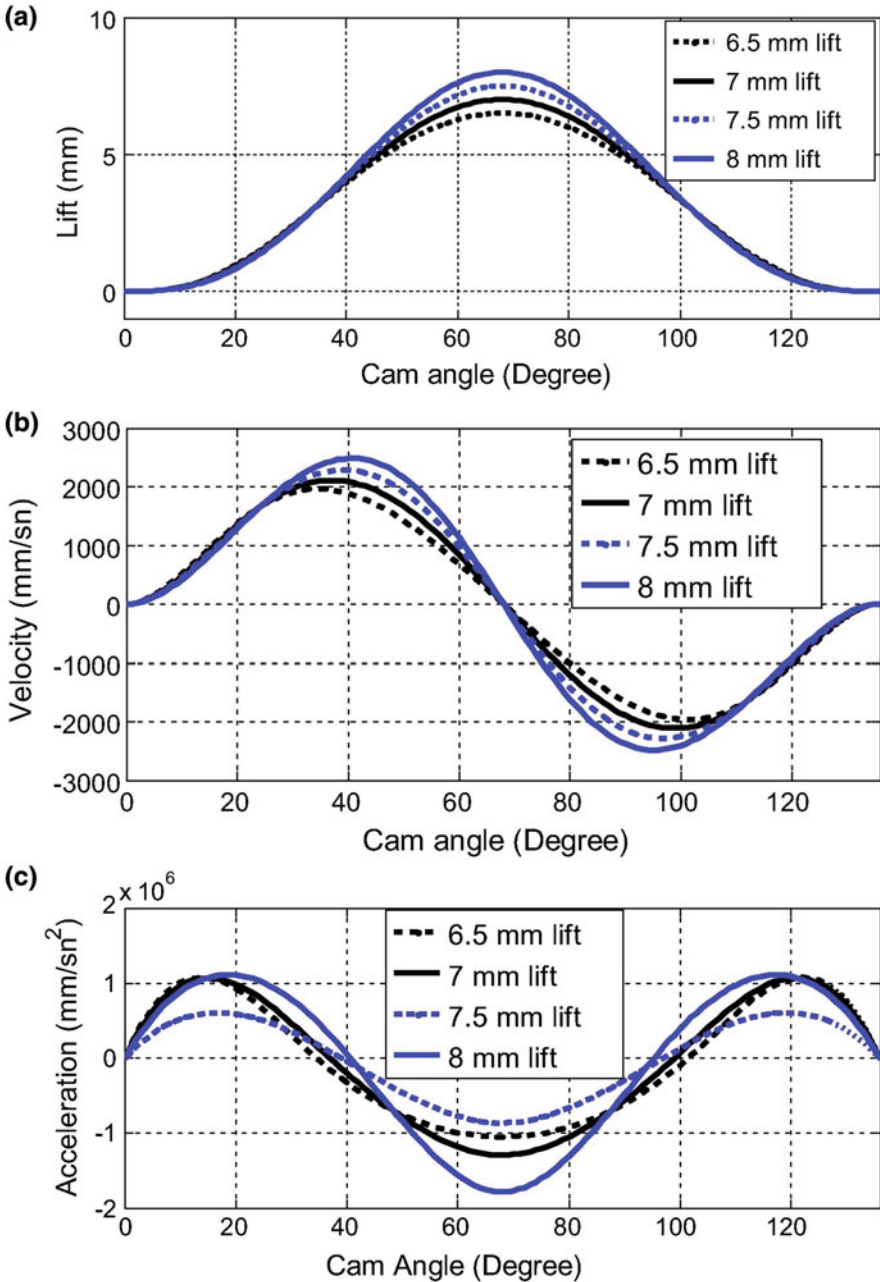


Fig. 3.19 Typical valve (a) displacement (lift), (b) velocity, and (c) acceleration curves as a function of cam position [26]

thus, similar technologies can be used for the measurement of valve displacement, namely, Hall effect, carrier frequency, and capacitive techniques with appropriate signal conditionings [2]. The recorded analog signals can be used to derive velocity and acceleration of reciprocating valve components. Figure 3.19 shows the typical valve lift, velocity, and acceleration profiles with respect to cam positions.

The analysis of the dynamic behavior of the valve train on motored test rigs has taken a firm position in the development of valve train components. However, influences caused by the gas exchange process, thermal effects, and additional issues of a complete engine under fired conditions are neglected with the motored approach. Thus, the differences between the ideal and real valve opening and closing together with real valve timing as well as detailed information about the gas exchange and the dynamic behavior of the valves need to be measured [25]. In order to measure the valve lift and velocity, typically a laser Doppler vibrometer (LDV) is used. The laser Doppler vibrometer is based on the principle of the detection of the Doppler shift of coherent laser light that is scattered from a small area of a test object. A study performed dynamic valve train investigations using LDV measurement on the motored test rig while on a fired engine using magneto-resistive (MR) sensors [25]. Magneto-resistive sensors are ideal for the position, speed, and angle detection. The signal of the sensors is generated by an external magnetic field with changing direction, which results into a change of the sensor's electrical resistance. If the sensor is mounted between a permanent magnet and a tooth structure of ferromagnetic material, the movement of this tooth structure deflects the magnetic field. The signal period characterizes the movement of the tooth structure. A linear relationship between the movement and the signal can be established for a particular tooth spacing.

3.7 Ignition Current Sensor

Ignition and combustion process in a gasoline or spark ignition engine are related by ignition signals. The timing of the ignition of the fuel-air mixture with respect to crankshaft position is critical for achieving the optimal fuel conversion efficiency. The ignition of the fuel-air mixture, the development of the flame front, and the combustion process must synchronize correctly with respect to the piston position and variations in-cylinder volume [2]. Therefore, the ignition timing has to be optimized and adjusted with respect to various engine operating parameters.

Ignition timing is defined as the exact instant a spark is sent to the spark plug. Spark timing is typically expressed in degrees of crankshaft rotation relative to TDC position. In most engines, the spark is designed to occur slightly before TDC due to the finite time that is taken for burning the fuel. If the ignition timing of an engine is not adjusted correctly, the spark may occur either before or after its best position. The early spark timings would result in difficult starting, poor performance, increased fuel consumption, and slow, rough idling. In later spark timing case, slow and jerky cranking with the warm engine may occur, and also some of the power strokes are wasted. Knocking may also be experienced while accelerating in



Fig. 3.20 Ignition time module and inductive pickup sensor (Courtesy of AVL)

early spark timings (depending on the amount of advanced spark timing). Therefore, it is very important to measure the exact ignition timing and calibrate according to system requirements [27]. Several factors affect the ignition timings including engine speed, type of fuel, mixture strength, and engine operating load. Direct measurement of ignition advance timing as well as absolute timing with respect to TDC is proposed for using directly on vehicles [27].

In a conventional ignition system, a high-tension voltage distribution to each cylinder via high-voltage cables and mechanical, high-voltage distributors is used. An inductive clamp can be used to capture the ignition timing signals. Figure 3.20 shows the commercially available ignition timing module along with an inductive pickup sensor. The module is available with an inductive current pickup that can be clamped onto the high-voltage cable of the particular cylinder for which ignition timing is measured.

The actual signal interface to the combustion measuring system depends on the type of ignition system. Typically, modern engines have a single ignition coil or one transformer per cylinder, and these are switched via a low-level on-off pulse. This pulse can be recorded on the combustion data acquisition system just by connecting the voltage signal through a suitable amplifier without any additional transducer [2]. The ignition time module can also detect and process lower-voltage signals coming, for instance, from the ECU, making the ignition time module suitable for any type of ignition systems (Fig. 3.20).

3.8 Sensors for Oxygen Detection and Air-Fuel Ratio Control

Air-fuel ratio plays an important role in the engine combustion process. Conventional spark ignition engine requires air-fuel ratio close to stoichiometric for sustaining the flame and complete flame propagation [8]. Typically, three-way catalytic

converter is used as aftertreatment technology to meet the emission legislation. For the effective operation of the three-way catalytic converter, the engine must operate at the stoichiometric air-fuel ratio. For meeting this condition ($\Phi \sim 1$), a closed-loop control of air-fuel ratio is applied. Measurement of the oxygen concentration in the exhaust is used to determine the air-fuel ratio in the cylinder charge. Figure 3.21 shows the typical functional principle of zirconium oxide-based oxygen sensor and its characteristic output signal.

The oxygen sensor consists of a zirconia (ZrO_2) ceramic solid electrolyte. The electrolyte acts as a catalyst, and it is placed between two noble metal (platinum)

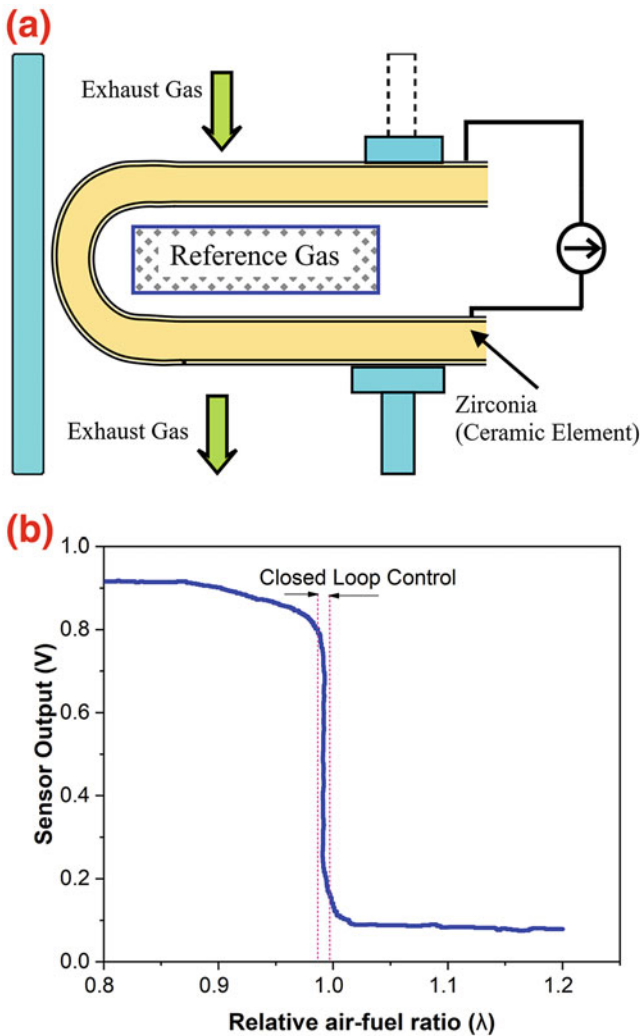


Fig. 3.21 (a) Typical functional principle of oxygen sensor and (b) characteristic output signal of oxygen sensor (Adapted from [9, 24, 28])

electrodes. The oxygen will flow from high partial pressure to low partial pressure when the partial pressure of oxygen is different at the two electrodes. The platinum electrode catalyzes the reversible reaction of oxygen disassociation and combination [28]. Oxygen from “air-side” (reference gas) of the sensor forms oxygen cations, which migrates across the zirconia to recombine and forming the oxygen. The potential difference created by ions is measured as an output voltage. The characteristic signal observed is shown in Fig. 3.21b. This sensor is only sensitive within a narrow λ range around $\lambda = 1$. Therefore, this signal is used as feedback for closed-loop combustion control of spark ignition engines.

The universal exhaust gas oxygen sensor (UEGO) is also developed to meet the wide range of air-fuel ratio control in lean-burn engines [9]. A UEGO sensor has a similar dimension to a lambda sensor. It is small and compact and can be easily installed in the engine exhaust. The UEGO sensor can be used to estimate the individual cylinder air-fuel ratio and closed-loop control of the engine [29, 30].

Discussion/Investigation Questions

1. Discuss the need for low-pressure (intake and exhaust manifold pressure) measurement for combustion and performance analysis of the engine. Write the characteristics required for the typical sensor used for the measurement of intake and exhaust pressure.
2. Discuss and list down the factor influencing the absolute pressure measurement and its dynamics in the intake and exhaust manifold in a modern engine.
3. Discuss the possible reasons for the use of adapters in inlet and outlet pressure measurement in modern engines. Comment on the best mounting position for the pressure sensor in the intake and exhaust manifold of the engine.
4. Discuss how low pressure (intake and exhaust) affects the combustion in SI, CI, and HCCI engines. Justify the importance of low-pressure measurement in three combustion modes.
5. Discuss the advantages provided by common rail direct injection (CRDI) technology over the distributor pump systems. Write the differences between the fuel pressure curves in the two fuel injection technologies.
6. Discuss the expected characteristics of a fuel pressure sensor for line pressure measurement in modern diesel engines.
7. Discuss the importance of the fuel line pressure and injector needle lift measurement. Write the information that can be generated by processing the signals acquired from line pressure and needle lift sensors. Draw the typical curves of these signals for CRDI and distributed pump engines.
8. Discuss how the opening phase of the injector needle (initial lift) affects the spray dynamics in modern diesel engines. Comment on the relation between needle lift and axial jet velocity of spray in CRDI engine.
9. Write the limitations of inductive (eddy-current)-based injector needle lift measurement in CRDI engines. Discuss one possible alternative for the needle lift

- measurement with better accuracy and repeatability than the inductive-based method in CRDI engines.
10. Discuss the role of air and fuel mass flow measurement on performance and combustion analysis of an engine. Write the equations relating combustion/performance parameter involving air or fuel mass flow rates. Discuss the possible ways of calculating air-fuel ratio at particular engine operating condition.
 11. Calculate the volume of air-box required for flow rate measurement in a single-cylinder four-stroke engine having a displacement volume of 500 cm^3 operated at 1500 rpm. Assume the diameter of orifice used measurement is 2.5 cm. Calculate the ratio of air-box volume and engine volume. What is the method you will suggest to reduce this ratio? Discuss the possible reasons why the higher volume of air-box is required at lower engine speeds and vice versa.
 12. Discuss the limitations of airflow measurement with air-box and discuss flow-meter methods. Explain a method for instantaneous air mass flow rate measurement.
 13. Discuss the reasons why gravimetric methods of fuel mass determination are preferred over the volumetric methods. Explain a volumetric and a gravimetric-based fuel mass flow rate determination in a diesel engine.
 14. Explain why it is essential to operate a conventional spark ignition (SI) engine on the stoichiometric air-fuel ratio. Discuss the method to control the air-fuel ratio in SI engines.
 15. Discuss the functional principle of the oxygen sensor (λ sensor) used in conventional SI engines. What are the possible methods for estimation of air-fuel ratio estimation in combustion engines? Comment on the merit of each method.

References

1. Czerwinski, J., Comte, P., Hilfiker, T., & Fürholz, A. (2012). *Research of techniques for low pressure indication in internal combustion engines* (No. 2012-01-0444). SAE Technical Paper.
2. Rogers, D. R. (2010). *Engine combustion: Pressure measurement and analysis*. Warrendale, PA: Society of Automotive Engineers.
3. Gossweiler, C., Sailer, W., & Cater, C. (2006). *Sensors and amplifiers for combustion analysis, A guide for the User 100-403e-10.06*, © Kistler Instrumente AG, CH-8408 Winterthur, Okt. 2006.
4. Van Basshuysen, R., & Schäfer, F. (2016). *Internal combustion engine handbook-basics, components, systems and perspectives* (2nd ed.). Warrendale, PA: SAE International.
5. Ueno, M., Izumi, T., Watanabe, Y., & Baba, H. (2008). *Exhaust gas pressure sensor* (No. 2008-01-0907). SAE Technical Paper.
6. Leach, F. C., Davy, M. H., Siskin, D., Pechstedt, R., & Richardson, D. (2017). An optical method for measuring exhaust gas pressure from an internal combustion engine at high speed. *Review of Scientific Instruments*, 88(12), 125004.
7. Vítek, O., & Poláček, M. (2002). *Tuned manifold systems-application of 1-D pipe model* (No. 2002-01-0004). SAE Technical Paper.
8. Maurya, R. K. (2018). *Characteristics and control of low temperature combustion engines: Employing gasoline, ethanol and methanol*. Cham: Springer.
9. Ladommatos, N., & Zhao, H. (2001). *Engine combustion instrumentation and diagnostics*. Warrendale, PA: SAE International.

10. Dhar, A. (2013). *Combustion, performance, emissions, durability and lubricating oil tribology investigations of biodiesel (karanja) fuelled compression ignition engine* (PhD thesis). IIT Kanpur.
11. Krogerus, T., Hyvönen, M., & Huhtala, K. (2018). Analysis of common rail pressure signal of dual-fuel large industrial engine for identification of injection duration of pilot diesel injectors. *Fuel*, 216, 1–9.
12. Payri, R., Gimeno, J., Viera, J. P., & Plazas, A. H. (2013). Needle lift profile influence on the vapor phase penetration for a prototype diesel direct acting piezoelectric injector. *Fuel*, 113, 257–265.
13. Margot, X., Hoyas, S., Fajardo, P., & Patouna, S. (2011). CFD study of needle motion influence on the exit flow conditions of single-hole injectors. *Atomization and Sprays*, 21(1), 31–40.
14. Wang, T. C., Han, J. S., Xie, X. B., Lai, M. C., Henein, N. A., Schwarz, E., & Bryzik, W. (2003). Parametric characterization of high-pressure diesel fuel injection systems. *Journal of Engineering for Gas Turbines and Power*, 125(2), 412–426.
15. Huang, W., Moon, S., & Ohsawa, K. (2016). Near-nozzle dynamics of diesel spray under varied needle lifts and its prediction using analytical model. *Fuel*, 180, 292–300.
16. Payri, R., Gimeno, J., Venegas, O., & Plazas, A. H. (2011). *Effect of partial needle lift on the nozzle flow in diesel fuel injectors* (No. 2011-01-1827). SAE Technical Paper.
17. Coppo, M., Dongiovanni, C., & Negri, C. (2004). Numerical analysis and experimental investigation of a common rail type diesel injector. *Journal of Engineering for Gas Turbines and Power*, 126, 874–885.
18. Coppo, M., Dongiovanni, C., & Negri, C. (2007). A linear optical sensor for measuring needle displacement in common-rail diesel injectors. *Sensors and Actuators A: Physical*, 134(2), 366–373.
19. Amirante, R., Catalano, L. A., & Coratella, C. (2013). *A new optical sensor for the measurement of the displacement of the needle in a common rail injector* (No. 2013-24-0146). SAE Technical Paper.
20. Kastner, L. J. (1947). An investigation of the airbox method of measuring the air consumption of internal combustion engines. *Proceedings of the Institution of Mechanical Engineers*, 157(1), 387–404.
21. Stone, R. (1992). *Introduction to internal combustion engines* (2nd ed.). London: MacMillan.
22. Martyr, A. J., & Plint, M. A. (2007). *Engine testing* (3rd ed.). Oxford: Butterworth-Heinemann (Elsevier).
23. Turner, J. (2009). Temperature sensors. In J. Turner (Ed.), *Automotive sensors* (pp. 85–105). New Jersey: Momentum Press.
24. Reif, K. (2015). *Gasoline engine management*. Friedrichshafen: Springer Vieweg.
25. Kerres, R., Schwarz, D., Bach, M., Fuoss, K., Eichenberg, A., & Wüst, J. (2012). Overview of measurement technology for valve lift and rotation on motored and fired engines. *SAE International Journal of Engines*, 5(2), 197–206.
26. Çinar, C., Şahin, F., Can, Ö., & Uyumaz, A. (2016). A comparison of performance and exhaust emissions with different valve lift profiles between gasoline and LPG fuels in a SI engine. *Applied Thermal Engineering*, 107, 1261–1268.
27. Aggarwal, S., Subbu, R., & Gilotra, S. (2015). *A new approach in measurement of ignition timing directly on a two-wheeler using embedded system* (No. 2015-01-1642). SAE Technical Paper.
28. Swingler, J. (2009). Gas composition sensors. In J. Turner (Ed.), *Automotive sensors* (pp. 231–257). New Jersey: Momentum Press.
29. Benvenuti, L., Di Benedetto, M. D., Di Gennaro, S., & Sangiovanni-Vincentelli, A. (2003). Individual cylinder characteristic estimation for a spark injection engine. *Automatica*, 39(7), 1157–1169.
30. Cavina, N., Corti, E., & Moro, D. (2010). Closed-loop individual cylinder air–fuel ratio control via UEGO signal spectral analysis. *Control Engineering Practice*, 18(11), 1295–1306.